Plant Physiology and Biochemistry 201 (2023) 107865

Contents lists available at ScienceDirect

Plant Physiology and Biochemistry

journal homepage: www.elsevier.com/locate/plaphy

Arabidopsis subtilases promote defense-related pectin methylesterase activity and robust immune responses to botrytis infection☆

Daniele Coculo [a], Daniele Del Corpo [a], Miguel Ozáez Martínez [b], Pablo Vera [b], Gabriella Piro [c], Monica De Caroli [c], Vincenzo Lionetti [a,d,*]

[a] Dipartimento di Biologia e Biotecnologie Charles Darwin, Sapienza Università di Roma, Rome, Italy
[b] Instituto de Biologia Molecular y Celular de Plantas, Universidad Politecnica de Valencia-C.S.I.C, Ciudad Politecnica de La Innovacion, Valencia, Spain
[c] Dipartimento di Scienze e Tecnologie Biologiche e Ambientali, Università Del Salento, Lecce, 73100, Italy
[d] CIABC, Sapienza Università di Roma, Rome, Italy

ARTICLE INFO

Keywords:
Pectin methylesterases
Subtilases
Plant immunity
Botrytis cinerea
Arabidopsis thaliana
Cell wall integrity

ABSTRACT

Plants involve a fine modulation of pectin methylesterase (PME) activity against microbes. PME activity can promote the cell wall stiffening and the production of damage signals able to induce defense responses and plant resistance to pathogens. However, the molecular mechanisms underlying PME activation during disease remain largely unknown. In this study, we explored the role of subtilases (SBTs) as PME activators in Arabidopsis immunity. By using biochemical and reverse genetic approaches, we found that the expression of SBT3.3 and SBT3.5 influences the induction of defense-related PME activity and resistance to the fungus *Botrytis cinerea.* Arabidopsis *sbt3.3* and *sbt3.5* knockout mutants showed decreased induction of PME activity and increased susceptibility to the fungus. *SBT3.3* expression was stimulated by oligogalacturonides. Overexpression of *SBT3.3* overactivated PME activity during fungal infection and enhanced resistance to *B. cinerea*. A negative correlation was observed between *SBT3.3* expression and cell wall methyl ester content in the genotypes analyzed after *B. cinerea* infection. Increased expression of defense-related genes, including *PAD3*, *CYP81F2* and *WAK2*, was also revealed in *SBT3.3* overexpressing lines. We also demonstrated that SBT3.3 and pro-PME17 are both secreted into the cell wall using distinct protein secretion pathways and different kinetics. Our results propose SBT3.3 and SBT3.5 as modulators of PME activity in Arabidopsis against Botrytis to promptly boost immunity limiting the growth-defense trade-off.

Author contributions

V.L. conceived the research; G.P, P.V and L.V. developed the experimental designs and supervised the experiments; D.C., D.D.C, M.O. M and M.D.C performed the experiments; D.C., M.D.C, G.P, P.V. and V.L. analyzed data; All authors contributed to discussing the results of this manuscript. V.L. wrote the article with contributions of all the authors.

1. Introduction

Plants continuously sense microbial attacks by eliciting a timely and effective immune response. Part of this recognition occurs through Pattern Recognition Receptors (PRRs) at plasma membrane that can detect Microbial-, Pathogen-, or endogenous Damage-Associated Molecular Patterns (MAMPs, PAMPs or DAMPs) (Zhou and Zhang, 2020). Pattern-triggered immunity (PTI) is the first line of plant-inducible immunity that restricts pathogen proliferation. Since the immunity efforts often result in a growth-defense trade-off, fine-tuning of immune pathways becomes critical to optimize plant fitness (Lionetti et al., 2010). Protease-mediated proteolysis plays a central role in this homeostasis and is widely implicated in plant stress, although its mechanism of action is still largely unknown (Hou et al., 2018). Phytocytokines such as Plant Elicitor Peptides (PEPs), (PAMP)-INDUCED PEPTIDES (PIPs) and SERINE-RICH ENDOGENOUS PEPTIDES (SCOOPs) are examples of peptides that are proteolytically released from larger precursors (pro-proteins) that emerged as fundamental regulators of innate immunity (Hou et al., 2021). Subtilases (SBTs, Pfam00082), serine peptidases belonging to family S8 (MEROPS database; https://www.ebi.ac.uk/merops/cgi-bin/famsum?family=S8), can

☆ One sentence Summary: Subtilases trigger pectin methylesterase activity and reinforce Arabidopsis immunity to Botrytis.

* Corresponding author. Dipartimento di Biologia e Biotecnologie Charles Darwin, Sapienza Università di Roma, Rome, Italy.
E-mail address: vincenzo.lionetti@uniroma1.it (V. Lionetti).

https://doi.org/10.1016/j.plaphy.2023.107865
Received 21 March 2023; Received in revised form 22 June 2023; Accepted 26 June 2023
Available online 13 July 2023

Abbreviations

BFA	Brefeldin A
CW	Cell Wall
DAB	3,3′-Diaminobenzidine
DAMPs	Damage Associated Molecular Patterns
ER	Endoplasmic Reticulum
EXPOs	Exocyst Positive Organelles
FER	FERONIA
Gal A	Galacturonic Acid
GFP	Green Fluorescent Protein
GPI	Glycosylphosphatidylinositol
HG	Homogalacturonan
H_2O_2	Hydrogen peroxide
MAMPs	Microbe Associated Molecular Patterns
MAPKs	Mitogen-activated protein kinases
MeOH	methanol
OGs	Oligogalacturonides
PAD	PHYTOALEXIN DEFICIENT
PAMPs	Pathogen Associated Molecular Patterns
PEPs	Plant Elicitor Peptides
PGs	Polygalacturonases
PIPs	(PAMP)-INDUCED PEPTIDES
PMEIs	PME Inhibitors
PMEs	Pectin Methylesterases
pro-PMEs	(pro region or PMEI-like domain) -PMEs
PRRs	Pattern Recognition Receptors
PTI	Pattern-triggered immunity
RALF	RAPID ALKALINIZATION FACTOR
SAMS	S-adenosylmethionine synthase
SBTs	Subtilases
SCOOPs	SERINE-RICH ENDOGENOUS PEPTIDES
VGD	VANGUARD
WAK	WALL-ASSOCIATED KINASE
XTH	Xyloglucan endotransglucosylase/hydrolase
YFP	Yellow Fluorescent Protein

process pro-proteins and play a key role in defense responses against microbes, plant parasitism, and adaptation to environmental changes (Schaller et al., 2018). In *A. thaliana,* 56 SBT isoforms are divided into 6 subfamilies: SBT1, SBT2, SBT3, SBT4, SBT5, SBT6. By cleaving multiple host proteins, SBTs could trigger in plants an activation cascade to generate and enhance the efficacy of warning signals, such as caspase in programmed cell death in mammals (Paulus and Van der Hoorn, 2019). In tomato, specific SBTs contribute to jasmonic acid-mediated resistance to *Manduca sexta* larvae by processing the wound pro-hormone prosystemin and releasing the bioactive peptide systemin (Meyer et al., 2016). Specific SBTs target the plant cell wall (CW), the foremost interface where plant-microbe interactions take place, to trigger specific defense signals. The six genes of the tomato cluster SBT P69 (P69A–P69F) encode proteins particularly involved in plant defense. P69C can process a leucine rich repeat protein associated with the extracellular matrix, the first physiological target of an extracellular SBT proposed in plants (Tornero et al., 1996). SBT3.3, the ortholog of P69C in Arabidopsis, was discovered as regulator of primed immunity against *P. syringae* and *Hyaloperonospora arabidopsidis* (Ramirez et al., 2013). Although SBT3.3 was postulated to cleave a larger extracellular protein, the identification of its specific substrate and the mechanism by which SBT3.3 can trigger immunity remain to be identified.

During plant development, SBTs can activate pectin methylesterases (PMEs; Pfam01095), enzymes regulating the methylesterification of Homogalacturonan (HG), the major constituent of pectin in the CW of dicotyledonous plants (Pelloux et al., 2007). PMEs catalyse the hydrolysis of methylester bonds at C-6 of galacturonic acid (Gal A) residues, producing acidic pectins with negatively charged carboxyl groups, releasing methanol (MeOH) and protons into the apoplast. In Arabidopsis, 66 PME isoforms can be divided into 2 groups according to their structure. Group 1 includes 21 PME isoforms, that contain only the catalytic domain. The 45 PME isoforms in Group 2 (hereafter referred to as pro-PMEs) are organized as a polycistronic messenger RNA resembling an operon-like gene cluster (Coculo and Lionetti, 2022). In pro-PMEs, the catalytic PME domain is preceded by an N-terminal region (also referred to as the pro region or PMEI-like domain) that shares structural similarities with functionally characterized PME inhibitors (PMEIs) and that can act as self inhibitor (Del Corpo et al., 2020). This PME domain could prevent premature de-methylesterification of pectin during specific steps of its secretion, assembly, or modification, thus contributing to its proper functionality. The Arabidopsis SBT3.5 can process pro-PME17, which releases PME activity during root growth in Arabidopsis seedlings (Senechal et al., 2014). SBT1.7 modulates PME activity in the release of mucilage from Arabidopsis seed coats (Rautengarten et al., 2008). AtSBT6.1 can process the pollen-specific PME VANGUARD1 (VGD1) suggesting its possible involvement in the pro-PME maturation during pollen tube formation (Wolf et al., 2009). The subtilisin-like protease SlSBT3 contributes to insect resistance in tomato (Meyer et al., 2016). Although SlSBT3 expression affected PME activity and the level of pectin methylesterification, these effects were unrelated to its role in herbivore defense.

Strong local induction of PME activity is exerted in *Arabidopsis thaliana* and other plants, when challenged with microbial pathogens (Lionetti, 2015). Specific PME isoforms showed significantly altered timing and expression level in *A. thaliana-B. cinerea* interaction and in many other pathosystems (Lionetti et al., 2012, 2017). Among them, *pro-PME17* is induced during infection of a wide range of plant pathogens and can be considered a general biomarker for pathogenesis. Recently, pro-PME17 was involved in triggering PME activity and resistance to *B. cinerea* (Del Corpo et al., 2020). The pro region acts as an intramolecular inhibitor of pro-PME17 activity. PME activity can serve multiple functions in plant immunity (Coculo and Lionetti, 2022). PMEs produce negatively charged carboxyl groups that may form consecutive calcium bonds with other HG molecules, thereby strengthening the CW by forming “egg-boxes” structures. PME activity may also promote DAMP-related immunity. In particular, the PME activity could favour the release and perception of de-methylesterified oligogalacturonides (OGs), DAMPs that are released locally in cooperation with endo-polygalacturonases (PGs), and are able to trigger plant immunity (Osorio et al., 2008). OGs are sensed in Arabidopsis by the WALL-ASSOCIATED KINASE1 (WAK1) PRR to activate immune responses (Brutus et al., 2010). WAK2 requires PME-mediated pectin de-methylesterification to activate OGs-dependent stress responses (Kohorn et al., 2014). Interestingly, WAK1, WAK2 and another PRR, FERONIA (FER), preferentially bind to de-methylesterified pectins (Lin et al., 2021). De-methylesterification of pectin can also represents the primary mechanism for generation of plant-derived methanol (MeOH), a DAMP-like warning signal (Dorokhov et al., 2012). OGs and MeOH could trigger a defensive priming effect that sets the stage for intra- and inter-plant immunity (Giovannoni et al., 2021).

Precise on/off mechanisms regulating PME activity appear to be necessary for an efficient defense response without compromising growth (He et al., 2022). The need for post-transcriptional control of PME activity by specific PME inhibitors (PMEIs) in the late stages of plant invasion by microbes has been previously demonstrated (Lionetti et al., 2017). The involvement of SBTs as PME activators in plant immunity to microbes has not yet been investigated. Here, we found that all PME isoforms induced in *A. thaliana* against the necrotrophic fungus

Botrytis cinerea possess a pro region. By exploiting reverse genetics and biochemical approaches, we demonstrated that expression of SBT3.3 and SBT3.5 affects PME activity in Arabidopsis immunity to Botrytis. Notably, we found that the expression of SBT3.3 can be activated by OGs and can affect CW methylesterification during *B. cinerea* infection. Overexpression of SBT3.3 overactivated specific defense-related genes, including WRKY33 and PAD3 involved in camalexin accumulation and WAK2 involved in maintaining pectin integrity. SBT3.3 and pro-PME17 follow distinct secretory pathways to reach the apoplast where they subsequently colocalize. Our results provide evidence that SBTs activate defense-related PME activity and pectin integrity signalling for a timely immune response.

2. Materials and methods

2.1. Plant, bacteria and fungus growth conditions

A. thaliana Wild-type Columbia (Col-0), *sbt* mutants and SBT3.3-OE seedlings were grown in solid 2.2 g L^{-1}Murashige and Skoog medium including vitamins (MS/2), 1% sucrose, 0.8% plant agar, pH 5.7 in a controlled environmental chamber maintained at 22 °C and 70% relative humidity, with a 16 h/8 h day/night cycle (PAR level of 100 μmol $m^{-2}s^{-1}$). Adult plants were transferred on soil in a growth chamber at 22 °C and 70% relative humidity under a 12 h/12 h day/night cycle (PAR level of 120 μmol $m^{-2}s^{-1}$). *Sbt* mutants used include SALK_086,092 (At1g32960; *sbt3.3–1*), SALK_107,460 (At1g32960; *sbt3.3–2*), SAIL_400_F09 (At1g32940; *sbt3.5–1*) and GABI_672C08 (At1g32940; *sbt3.5–2*). All mutants are in Col-0 background and are T-DNA insertion lines obtained from the Nottingham Arabidopsis Stock Centre (NASC).

Nicotiana tabacum cv SR1 seeds were sterilized using commercial grade bleach solution in the presence of 0.1% (v/v) for 15 min at room temperature and then washed three times for 5 min with distilled water before sowing. Seeds were germinated in a growth room at 25 °C and 30% relative humidity under a 16 h/8 h day/night cycle (photosynthetic photon flux of 50 μmol $m^{-2}s^{-1}$). Three-to four-week-old plants from MS medium were transferred on soil and grown in a controlled environment at 25 °C and 40% relative humidity under a 16 h/8 h day/night cycle (photosynthetic photon flux of 120 μmol $m^{-2}s^{-1}$). *Escherichia coli* TOP10 cells was grown in LB agar plate (Luria-Bertani: tryptone 1%, yeast extract 0.5%, NaCl 1%) containing ampicillin 50 μg/mL and incubated overnight at 37 °C. *Agrobacterium tumefaciens* (Strain GV3110) was grown in LB medium (Luria-Bertani: tryptone 1%, yeast extract 0.5%, NaCl 1%) containing appropriate antibiotics (Rifampycin 100 μg/mL and Spectomycin 100 μg/mL or Kanamycin 50 μg/mL) and incubated for 2 days at 28 °C. *B. cinerea* strain SF1 (Lionetti et al., 2007) was grown for 20 days on Malt Extract Agar at 20 g L^{-1} with Mycological Peptone at 10 g L^{-1} (MEP) at 23 °C and 70% relative humidity in the dark before conidia collection.

For seed germination analysis, *A. thaliana* WT, *sbt* mutants and SBT3.3-OE seeds were washed in 2 mL of isopropanol for 30 s followed by washing in 2 mL of sterile water for 3 min in slow stirring. The seeds were treated with 2 mL of sterilization solution (400 μl NaClO, 1.6 mL sterile water) for 5 min in slow agitation, followed by 4 washing steps in 2 mL of sterile water. For seed germination assay, triplicate sets of 60–70 sterilized seeds for each genotype were sown in Petri dishes on solid MS/2 medium in a controlled environmental chamber maintained at 22 °C and 70% relative humidity, with a 16 h/8 h day/night cycle (PAR level of 100 μmol m-2s-1). Seeds germination rate, as the number of germinated seeds divided by the total amount of seeds, was evaluated at 24, 48 and 72 h.

2.2. Genotyping of T-DNA insertion mutants

Genomic DNA was extracted using RBC Bioscience Genomic DNA Extraction Kits, according to the manufacturer's instructions, from leaves of 4-week-old Arabidopsis mutant and wild-type plants and subjected to a PCR-based screening using primer sequences described in Supplemental Table S1, generated with Primer3. Taq Kapa DNA Polymerase (Kapa Biosystem) was used at 1 units/30 μL. Amplification was performed in the presence of dNTPs (0.2 mM), 2.5 mM $MgCl_2$ and specific primers (10 μM) in the 1× buffer provided by the supplier. The conditions for amplification were 95 °C for 3 min; 36 cycles of amplification: 95 °C for 30 s, 60 °C for 30 s, 72 °C for 60 s, and a final extension of 72 °C for 1 min. The PCR products were separated by agarose gel electrophoresis and visualized by ethidium bromide staining. Plants homozygous for the mutations were propagated and used for all subsequent experiments.

2.3. Stable transformation of SBT3.3-OE Arabidopsis plants

Flowering Arabidopsis *sbt3.3-1* plants were transformed by floral dipping for 15 s in 200 mL of the culture medium with the inoculum of *Agrobacterium tumefaciens* C58 carrying the construction of interest. The plants were subsequently covered for 1 day to promote infection. The culture medium for immersion was composed of 2.2 g/L MS and 5% sucrose (w/v), supplemented with 0.005% Silwet and 0.05 μg/mL BAP. Selections of the 35 S::SBT3.3 homozygous transgenic plants were carried out on plates of MS medium supplemented with BASTA.

2.4. A. thaliana infection with Botrytis cinerea

Conidia of *B. cinerea* were harvested by washing the surface of the mycelium with sterile distilled water. Conidia suspensions were filtered to remove residual mycelium and the conidia concentration was determined using a Thoma chamber. Fully developed leaves from 4-week-old *A. thaliana* plants were infected with 1×10^6 conidia mL^{-1} incubated in Potato Dextrose Broth (PDB) at 24 g L^{-1}. Six droplets of spore suspension (5 μL each) were placed on the surface of each leaf. Mock inoculation was performed using PDB. Plants were incubated at 24 °C with a 12 h/12 h day/night photoperiod. The lesion size produced by *B. cinerea* was evaluated as an indicator of susceptibility to the fungus.

2.5. Elicitor treatment and gene expression analysis

B. cinerea-infected or mock-inoculated leaves were frozen in liquid nitrogen and homogenized using the mixer mill MM301 (RETSCH) and using stainless steel beads (5 mm in diameter) for about 1 min at 30 Hz. Total RNA was extracted with Isol-RNA Lysis Reagent (5′-Prime) according to the manufacturer's instructions. RNA was treated with RQ1 DNase (Promega), and first-strand complementary DNA (cDNA) was synthesized using ImProm-II reverse transcriptase (Promega). Quantitative Reverse Transcription PCR analysis was performed using a CFX96 Real-Time System (Bio-Rad). One microliter of cDNA (corresponding to 50 ng of total RNA) was amplified in 20 μL of reaction mix containing 1 × Go Taq qPCR Master Mix (Promega) and 0.5 μM of each primer described in Supplemental Table S2. The conditions for amplification were 95 °C for 2 min; 46 cycles of amplification: 95 °C for 15 s, 58 °C for 15 s, and a final extension of 72 °C for 15 s. The expression levels of each gene, related to the UBIQUITIN5 (UBQ5) gene, were determined using the Pfaffl method. Primer sequences were generated with Primer3 software (https://primer3.ut.ee/). Unbranched Oligogalacturonides (OGs) with a degree of polimerization (DP) 10 to 15 were generated by digesting polygalacturonic acid (PGA; Alfa Aesar) with an *Aspergillus niger* endopolygalacturonase (a gift from Prof. Jaap Visser, Wageningen University) as previously described (Pontiggia et al., 2015). 10-days-old Arabidopsis seedlings grown in liquid MS/2 medium were treated for 1 h with OG_S (40 μg mL^{-1}) or water as control, harvested and processed for RNA extraction as described above.

2.6. Determination of PME activity, fungal diffusion and H_2O_2 accumulation

Total protein extracts were obtained by homogenizing uninfected and infected Arabidopsis leaves in the presence of 1 M NaCl, 12.5 mM Citric Acid, 50 mM Na_2HPO_4, 0.02% Sodium Azide, protease inhibitor 1:200 v/v (P8849, Sigma), pH 6.5. Each sample was resuspended in 500 μL of protein Extraction Buffer. The homogenates were shaken for 3 h at 4 °C, centrifuged at 13.000×*g* for 15 min, and the supernatant (400 μL) collected. Protein concentration was determined in the supernatants using Bradford protein assay method (Bradford reagent, Sigma–Aldrich), a standard curve was performed using BSA (bovin serum albumine) at 1 mg mL^{-1}. PME activity was evaluated by using PECTOPLATE assay (Lionetti, 2015). PECTOPLATE was prepared with 0.1% (w/v) of apple pectin (molecular weight range 30,000–100,000 Da; 70–75% esterification; 76,282, Sigma-Aldrich, St. Louis), 1% (w/v) SeaKem® LE agarose (Lonza, Basel, Switzerland, Catalog no: 50004 E), 12.5 mM citric acid and 50 mM Na_2HPO_4, pH 6.5. Equal amounts of protein samples (2 μg of total protein in 20 μL) were loaded in each well of PECTOPLATE. Plates were incubated at 30 °C for 16 h, and stained with 0.05% (w/v) Ruthenium Red (RR) (R2751; Sigma-Aldrich, St. Louis) for 30 min. The plates were de-stained by several washes with water and the area of the fuchsia-stained haloes, resulting from de-methylesterification of pectin and the area of inner unstained haloes, resulting from the hydrolysis of pectin in the gel, were measured with ImageJ software. Known amounts of commercially available PME from orange (Citrus spp.) peel (P5400; Sigma-Aldrich) was used in the PECTOPLATE to generate a standard curve used to calculate PME activity in the protein extracts.

For the detection of *B. cinerea* hyphae, detached leaves were incubated for 30 min in lactophenol Trypan Blue solution (water: glycerol: lactic acid: phenol [1:1:1:1] + Trypan Blue solution [1 mg mL^{-1}; Sigma-Aldrich]). Thereafter, leaves were washed for overnight with gentle agitation in absolute ethanol to remove chlorophyll. Leaves were assayed for H_2O_2 accumulation employing 3,3′-diaminobenzidine staining as previously described (Reem et al., 2016). Leaves were mounted in 50% glycerol and examined by light microscopy using Nikon eclipse E200 microscope. Images were taken with a Nikon Digital Sight DS-Fi1c camera.

2.7. Determination of CW monosaccharide composition and methylester content

Extraction of alcohol-insoluble residue, CW monosaccharide composition and the determination of CW methylesters were performed as previously described (Lionetti et al., 2017).

2.8. SBT3.3-YFP and PME17-GFP/RFP gene constructs

For the SBT3.3-YFP overexpressing construct, a full-length cDNA for SBT3.3 was amplified by PCR using Pfu DNA polymerase (Stratagene, San Diego, CA) and specific primers, described in Supplemental Table S3, including Gateway adapters: BP SBT3.3 FW and BP SBT3.3 RV and recombined into pDONR207 using BP ClonaseMixII kit (Invitrogen). After sequencing, the construct was recombined with pB7FWG2 destination vector (YFP in C-terminal) using LR ClonaseMixII kit (Invitrogen). For pro-PME17-GFP/RFP overexpressing constructs, the full-length cDNA for pro-PME17 was amplified by PCR using *TakaRa* Ex Taq DNA polymerase (TAKARA, Kyoto), and specific primers flanked by Gateway adapters, attB sequences, described in Supplemental Table S3. PCR amplified attB-flanked DNA was recombined into pDONR221 using BP ClonaseMixII kit (Invitrogen). Specific pDESTs, pK7FWG2 and pK7RWG2,0, were used for GFP and RFP fusion in C-terminus to obtain pro-PME17-GFP and pro-PME17-RFP, respectively. All constructs were checked by sequencing (Eurofins Genomics, https://eurofinsgenomics.eu/). The Gateway constructs (pro-PME17-GFP, pro-PME17-RFP, SBT3.3-YFP, SBT3.3-mCherry) and RFP-HDEL, ST52-mCherry, XTH11-RFP, pm-rk and Exo70E2-mCherry were introduced into *Agrobacterium tumefaciens* (Strain GV3110) and the agroinfiltration was performed in *Nicotiana tabacum* leaves as previously described (De Caroli et al., 2011).

2.9. Transient transformation of Nicotiana tabacum leaves and confocal laser scanning microscopy

Almost fully expanded *Nicotiana tabacum* 6-week-old leaves were infiltrated with a suspension of *Agrobacterium tumefaciens* bearing the relevant construct in 2 mM Na_3PO_4; 50 mM 2-(N-morpholine)-ethanesulphonic acid (MES); glucose 0.5%; acetosyringone 100 μM; pH = 5.6 at an OD_{600} = 0.5. After 48- and 60-h post transformation (hpt) fluorescence was analyzed in infiltrated leaves by confocal microscopy. For co-infiltration, *Agrobacterium* cultures grown separately were adjusted to an OD_{600} = 0.5 and mixed prior to infiltration. For BFA (Sigma-Aldrich, http://www.sigmaaldrich.com) treatment, disks (1 cm diameter) of transformed leaves were treated by immersion in a solution of BFA at the final concentration of 100 μM. Plasmolysis was induced by incubating leaf disks in 1 M NaCl hypertonic solution for 10 min. Transiently transformed tobacco leaves were observed using a confocal laser scanning microscope LSM710 Zeiss (http://www.zeiss.com) mounting material in water as previously described (De Caroli et al., 2011). GFP and YFP were detected within the short 506–541 nm wavelength range, assigning the green color; RFP and mCherry were detected within 590–630 nm, assigning the red color. Excitation wavelengths of 488 and 543 nm were used. The laser power was set to a minimum and appropriate controls were made to ensure there was no bleed-through from one channel to the other. Images were processed using PHOTOSHOP7.0 (Adobe, https://www.adobe.com). For quantitative colocalization analyses, the overlap coefficient (OC, after Manders) and the Pearson's correlation coefficient (R) were evaluated as previously reported (De Caroli et al., 2011).

2.10. Bioinformatics tools

The Expression Angler tool of the Bio-Analytic Resource for Plant Biology (BAR, http://bar.utoronto.ca/welcome.htm) was used for co-expression analysis. E-plant (https://bar.utoronto.ca/eplant/) was used for to study developmental map and biotic stresses. Chromas was used to manage both nucleotide sequences and amino acids (https://chromas.software.informer.com/2.5/). Primer3 (https://primer3.ut.ee/) was used to design primers respectively for Gene expression analysis and Genotyping analysis. ImageJ (http://imagej.nih.gov/ij/download.html) was used to calculate the area of the haloes in PECTOPLATE assay. DNAMAN software (Lynnon, BioSoft, Quebec, Canada, https://www.lynnon.com/) was used for amino acid sequence analyses. Genevestigator Meta-Analyzer Tools (www.genevestigator.ethz.ch/at/) was used to analyze *SBT3.3* and *SBT3.5* gene expression during infection of Arabidopsis with different pathogens, DAMPs and PAMPs treatments.

2.11. Data analysis

Data were statistically analyzed and plotted into figures using GraphPad Prism 8.0.1 (GraphPad Software, San Diego, CA, USA). Data were presented as mean ± standard deviation (SD) or standard error (SE) as indicated in the figure legends. The significant differences were evaluated by ANOVA analysis followed by Tukey's test ($P < 0.05$).

2.12. Accession numbers

The genes used in this study have the following accession numbers: SBT3.3, At1g32960; SBT3.5, At1g32940; UBQ5, At3g62250; PAD3, At3g26830; CYP81F2, At5g57220; PME17, At2g45220; PMEI10, At1g62760; WAK2, At1G21270; At2g38470, WRKY33. *B. cinerea* β-tubulin, MG949129.1.

3. Results

3.1. In silico analysis implicated pro-PMEs and SBTs in plant immunity

After careful sequence comparison, we found that all Arabidopsis PME isoforms induced during *B. cinerea* infection are zymogens, expressed as inactive pro-PME precursors (Supplemental Fig. S1). Interestingly, while the PME catalytic domain is highly conserved, we revealed variability in the processing motif between the different defense-related PME isoforms. pro-PMEPCRA, pro-PME17 and pro-PME21 showed an RKLL processing motif, whereas the RRKL motif characterized the pro-PME20 and pro-PME41 isoforms. Instead, two

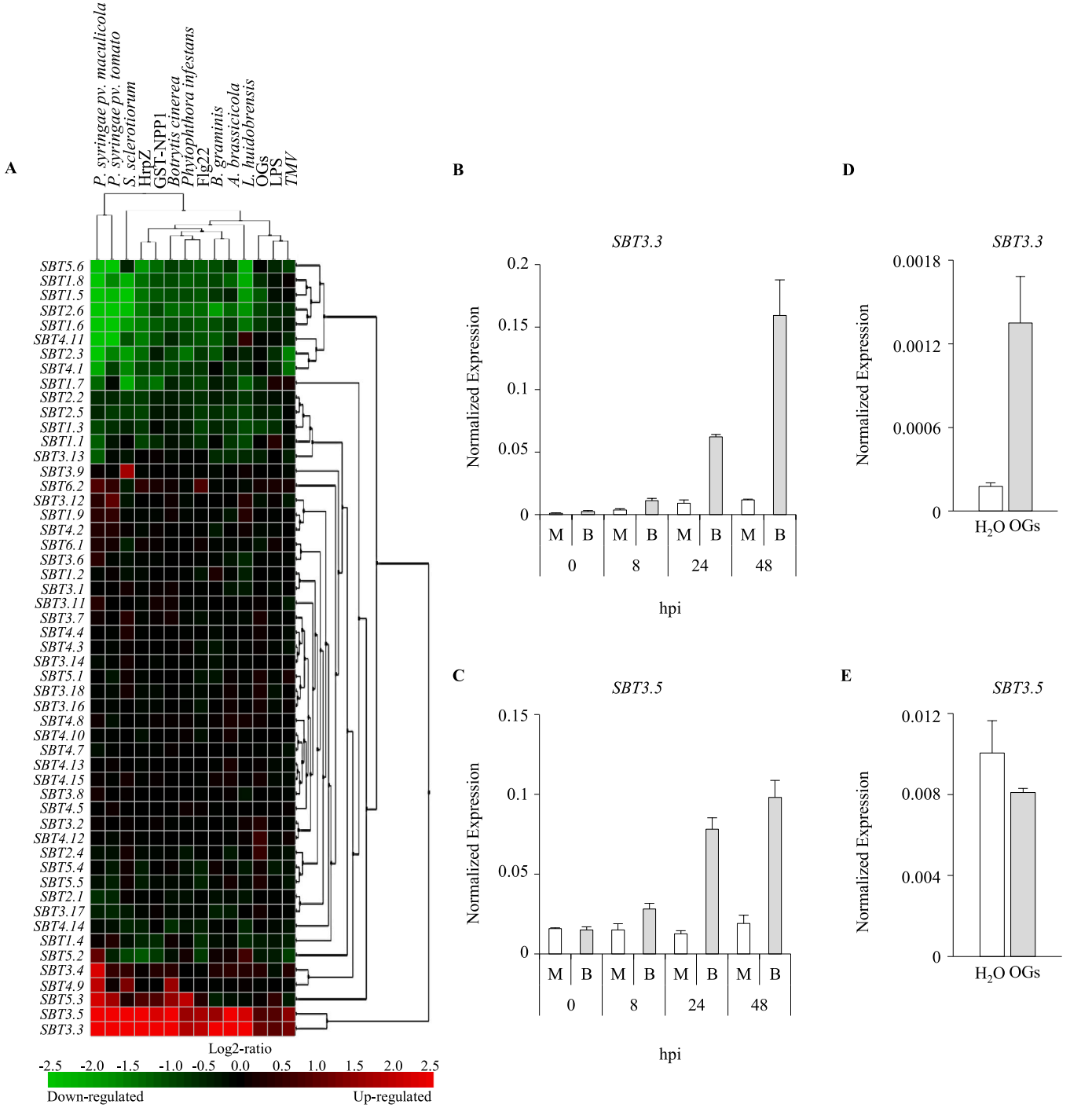

Fig. 1. *SBT3.3* and *SBT3.5* are induced in Arabidopsis during pathogen infection and in response to elicitor treatments. A) Clustering analysis of mRNA expression of SBTs in Arabidopsis challenged with different pathogens and in response to elicitors derived from bacteria (LPS, HrpZ, Flg22), oomycetes (GST-NPP1) and plants (OGs). Expression data were analyzed using the Genevestigator Meta-Analyzer Tools (www.genevestigator.ethz.ch/at/). The corresponding n-fold (log2 normalized) expression in infected plants is shown. Clustering analysis was performed using Euclidean distance with optimal leaf-ordering. **B)** *SBT3.3* and **C)** *SBT3.5* expression was analyzed in *B. cinerea* infected or mock-inoculated leaves at the indicated hours post inoculation (hpi) by qPCR. M = mock inoculated leaves. B = *B. cinerea* inoculated leaves. The expression of **D)** *SBT3.3* and **E)** *SBT3.5* was analyzed in Arabidopsis WT seedlings after 1 h of treatment with OGs or with water (H_2O) as control. Expression levels were normalized to *Ubiquitin5* expression. Data represent mean ± SD (n = 3). The experiments were repeated three times with similar results.

processing motifs, RKLK and RRLL were present in pro-PME3. Other motifs with the consensus sequence FPSW and LPLKMTERARAV are partially conserved between the isoforms. All these observations could imply the involvement of multiple protease-PME pairs. We next explored the possibility that SBTs are involved in the activation of pro-PMEs against microbes. Exploiting publicly available microarray data, the expression of the Arabidopsis SBTs isoforms (53 available isoforms out of 56) was analyzed after infection with several plant pathogens that differ in their lifestyle such as the necrotrophic fungi *B. cinerea, Sclerotinia sclerotiorum* and *Alternaria brassicicola*, the hemibiotrophic oomycete *Phytophtora infestans*, the biotrophic ascomycete *Blumeria graminis*, the biotrophic bacterium *Pseudomonas syringae*, the insect *Liriomyza huidobrensis* and tobacco mosaic virus (Fig. 1A). The response to bacterial-(LPS, HrpZ, Flg22), oomycete-(GST-NPP1) and plant-(OGs) elicitors was also investigated. Surprisingly, there are two isoforms, *SBT3.3* and *SBT3.5,* which are mainly expressed against all analyzed pathogens and in response to different elicitors. Interestingly, both genes are co-expressed with *pro-PME17* during Arabidopsis-Botrytis interaction (Supplemental Fig. S2). *SBT3.4*, *SBT4.9* and *SBT5.3* isoforms also appear to be modulated in specific pathosystems. It is also interesting to note the existence of gene clusters containing *SBTs* that are repressed upon biotic stresses.

3.2. SBT3.3 and SBT3.5 are induced in Arabidopsis against B. cinerea as part of PTI

To confirm the transcriptomic analysis and to gain more insight on the expression kinetics of these genes during disease, the expression levels of *SBT3.3* and *SBT3.5* were quantified at different time points in *B. cinerea*-infected and mock-inoculated *A. thaliana* wild type (WT) leaves by qPCR (Fig. 1B and C). *SBT3.3* was expressed only in infected tissues while *SBT3.5* showed basal expression also in mock-inoculated leaves. *SBT3.3* and *SBT3.5* were significantly induced at 24 hpi and further increased at 48 hpi, when they showed about 15- and 5-fold significant induction, respectively, in infected leaves compared to mock inoculated tissues. These data reveal an involvement of *SBT3.3* and *SBT3.5* in Arabidopsis-Botrytis interaction. We next investigated whether pectin-related DAMPs can impact the expression of selected SBTs. WT Arabidopsis seedlings were treated with OGs or water and the expression of *SBT3.3* and *SBT3.5* was evaluated at 1 h post treatment. A 7-fold induction of *SBT3.3* was revealed (Fig. 1D), while the expression of *SBT3.5* was not induced (Fig. 1E). Overall, these results indicate that *SBT3.3* and *SBT3.5* are part of Arabidopsis immune responses to *B. cinerea*.

3.3. Arabidopsis sbt3.3 and sbt3.5 mutants showed reduced PME activation and resistance to B. cinerea

To explore the possibility that SBT3.3 and SBT3.5 are involved in the activation of pro-PMEs in plant immunity, we exploited a reverse genetic approach. Two T-DNA insertional mutants were isolated for the selected genes (Fig. 2A). The insertions were in the fifth and ninth exons of the *sbt3.3–1* (SALK_086,092) and *sbt3.3–2* (SALK_107460.45.45) mutants, respectively, and in the first exon and second intron of the *sbt3.5–1* (SAIL _400_F09) and *sbt3.5–2* (GABI _672C08) mutants, respectively. The expression levels of SBT3.3 and SBT3.5 were compared in leaves of mutants and WT plants after *B. cinerea* and mock inoculation by qPCR (Fig. 2B). All mutants failed to induce gene expression in fungus-infected leaves, indicating that they are *sbt3.3* and *sbt3.5* KO lines. No significant defects in rosette growth and seed germination were observed in the *sbts* mutants, which have similar growth parameters as the WT plants (Fig. 2C and Supplemental Figs. 3A and B). To understand whether the lack of *SBTs* expression can influence pectin composition we compared the monosaccharide composition of matrix polysaccharides extracted from rosette leaves of *sbts* mutants and WT plants. All the mutants analyzed showed a molar percentage of monosaccharides not significantly different from that observed in WT plants (Fig. 2D).

Having established that the two SBTs are involved in Arabidopsis-Botrytis interaction we evaluated their possible contribution on the PME activity induced during fungal infection. The level of PME activity was quantified in leaves of WT, *sbt3.3–1*, *sbt3.3–2, sbt3.5–1* and *sbt3.5-2* plants at 24 h post Botrytis and mock inoculation (Fig. 3A). Significantly lower induction of PME activity was observed in infected *sbt3.3–1*, *sbt3.3–2*, *sbt3.5–1* and *sbt3.5-2* mutants (3.7-, 3.1-, 1.9-, and 1.8-fold reduction, respectively) compared with WT (Fig. 3A). These results indicate that *SBT3.3* and *SBT3.5* expressions influence PME activity in Arabidopsis immunity to Botrytis. The significant difference between *sbt3.3* and *sbt3.5* mutants suggests that the two proteases might activate different pro-PMEs isoforms during disease. No significant differences in PME activity were observed between mock-inoculated WT plants and *sbt* mutants. This was expected for *sbt3.3* mutants, because *SBT3.3* is not basally expressed in leaves (see mock in Figs. 1B and 2B). In *sbt3.5* mutants, the lack of the basal *SBT3.5* expression did not significantly affect monosaccharide composition and total PME activity in leaves (Figs. 2D and 3A) or rosette growth and seed germination (Fig. 2C and Supplemental Fig. S3). Therefore, we evaluated the susceptibility of *sbt3.3* and *sbt3.5* mutants to *B. cinerea* (Fig. 3B and C). Local fungal symptoms were significantly higher in both *sbt3.3* and *sbt3.5* mutants than in WT. The lesion areas caused by the fungus were greater in the *sbt3.3–1*, *sbt3.3–2*, *sbt3.5–1*, and *sbt3.5-2* mutants (by 2.2, 2.1, 1.7, and 1.7 times, respectively) compared to WT. Greater Botrytis mycelial development was detected in *sbt* mutants compared to WT plants by trypan blue staining (Fig. 3C). The results suggest that both SBTs contribute to trigger PME activity and Botrytis resistance, albeit to different extents. A correlation between the degree of resistance and the level of PME activity in the tissues was observed for the genotypes studied.

3.4. Overexpression of SBT3.3 overactivates defense related PME activity and restrict Botrytis infection

Given the lower induction of PME activity observed in *sbt3.3* mutants compared with *sbt3.5* mutants, we deepened our study by exploring the effect of *SBT3.3* overexpression in Arabidopsis on PME activity and Botrytis resistance. Two transgenic Arabidopsis lines, named *SBT3.3-OE1* and *SBT3.3-OE2* exhibiting high level of *SBT3.3* expression in leaves were characterized (Fig. 4A). An 85- and 90-fold overexpression was revealed, in leaves of *SBT3.3-OE1* and *SBT3.3-OE2* lines respectively, compared with WT when infected with *B. cinerea*. No growth abnormalities were observed in *SBT3.3* overexpressing plants (Fig. 4B and Supplemental Fig. S3). CW monosaccharide composition in rosette leaves of *SBT3.3-OE* lines was not significantly different from that quantified in WT plants (Fig. 4C). These results are consistent with those of the mutants and corroborate the conclusion that the expression of *SBT3.3* is strongly involved in the Arabidopsis immune response against the fungal infection. The level of PME activity was quantified in leaves of WT, *SBT3.3OE-1* and *SBT3.3OE-2* plants at 24 h post Botrytis- or mock-inoculation (Fig. 5A). A significantly higher induction of defense related PME activity was observed in infected *SBT3.3* overexpressing lines compared to control. *SBT3.3OE-1* and *SBT3.3OE-2* lines showed a 3.1- and 2.3- fold increase of PME activity, respectively, in the *B. cinerea* infected leaves compared to WT. Despite the *SBT3.3* overexpression in transgenic mock-inoculated plants, the level of PME activity was not significantly different from that measured in WT plants. This result highlights that the expression of *SBT3.3* promotes PME activity when Arabidopsis is challenged by the fungus.

Next, we evaluated the susceptibility of *SBT3.3-OE* lines to *B. cinerea*. Local symptoms of the fungus were significantly lower in both *SBT3.3-OE* plants than in WT (Fig. 5B). The area of lesions caused by the fungus was 2 and 1.5 times smaller in *SBT3.3-OE1* and *SBT3.3-OE2* lines, respectively, compared to WT. Less development of Botrytis mycelium was detected in *SBT3.3-OE1* plants respect to WT plants by trypan blue

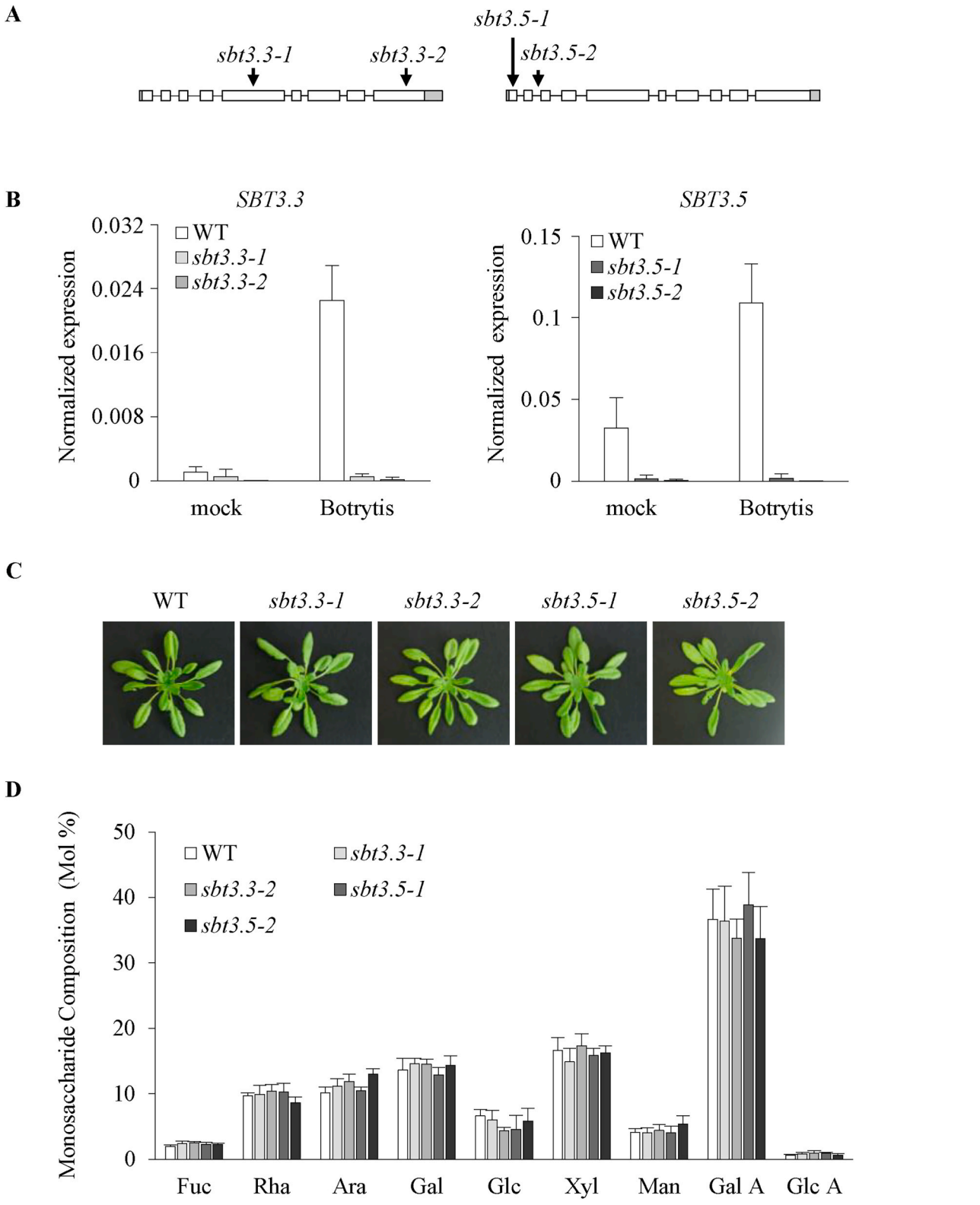

Fig. 2. Isolation of Arabidopsis *SBT3.3* and *SBT3.5* T-DNA insertional mutants. A) Schematic representation of *SBT3.3* and *SBT3.5* gene structures. The localization of T-DNA insertions in the gene sequences is shown (black arrows). 5′-UTR and 3′-UTR are represented in grey, exons in white and introns as a black line. **B)** The expression of *SBT3.3* and *SBT3.5* was analyzed in the respective mutants and WT plants at 24-h post inoculation with *B. cinerea*. Expression levels were normalized to *Ubiquitin 5* expression. The experiments were repeated three times with similar results. **C)** Representative pictures illustrating the morphology of vegetative rosettes of *sbt3.3* and *sbt3.5* mutants compared to WT. **D)** The monosaccharide composition of cell wall matrix polysaccharides was compared in leaves of *sbt3.3* and *sbt3.5* mutants and WT plants. The molar percentages of Fucose (Fuc), Rhamnose (Rha), Arabinose (Ara), Galactose (Gal), Glucose (Glu), Xylose (Xyl), Mannose (Man), Galacturonic Acid (Gal A) and Glucuronic Acid (Glc A) were quantified. Results represent the mean ± SD ($n \geq 3$). Monosaccharide datasets are not significantly different based on analysis of variance (ANOVA) followed by Tukey's test ($P < 0.05$).

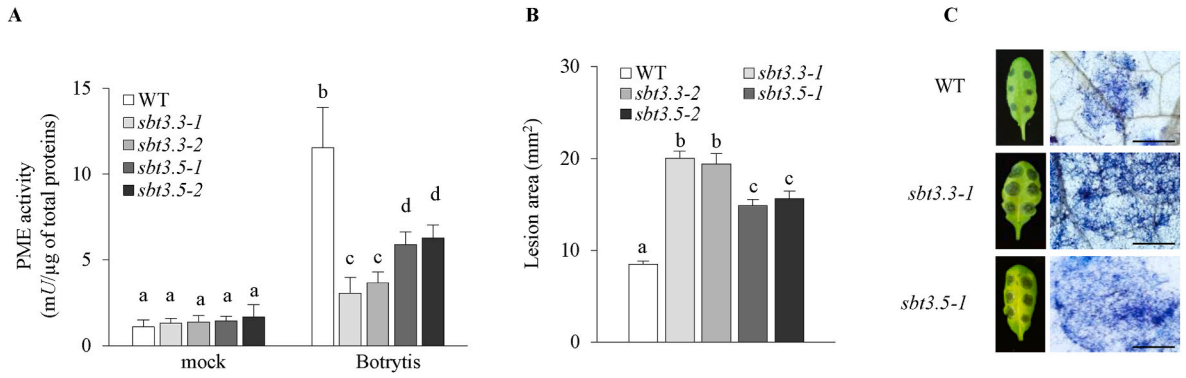

Fig. 3. Arabidopsis *sbt3.3* and *sbt3.5* mutants are defective in defense related PME activity and resistance against Botrytis. A) Leaves of Arabidopsis WT and of *sbt* mutants were inoculated with Botrytis and mock and PME activity was quantified at 24-h post inoculation (hpi). Results represent the mean ± SD (n = 6). **B)** Quantification of lesion areas produced by the spread of the fungus 24 h post infections. Data represent mean ± SE (n ≥ 36 lesions for each genotype). The different letters on the bars in B and C indicate significantly different datasets according to ANOVA followed by Tukey's test ($P < 0.05$). **C)** Photographs showing areas of lesions produced by Botrytis on leaves of WT, *sbt3.3–1* and *sbt3.5-1* mutants (left) and photomicrographs showing Botrytis colonization revealed by trypan blue staining (right). Bars = 1 mm.

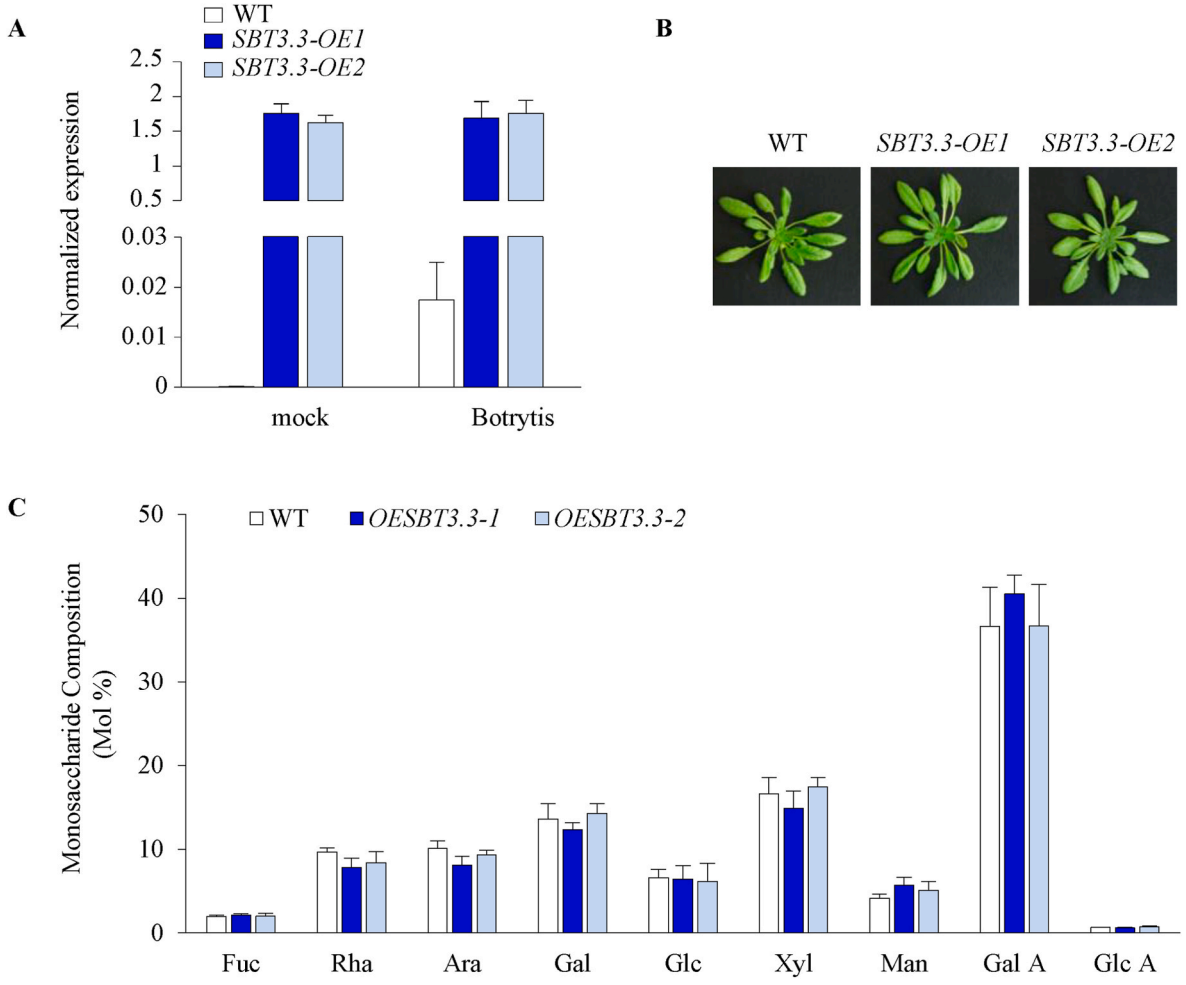

Fig. 4. Overexpression of SBT3.3 in Arabidopsis does not alter rosette growth and cell wall composition. A) *SBT3.3* expression was analyzed in the *SBT3.3-OE1* and *SBT3.3-OE2* transgenic plants at 24-h post inoculation with mock and *B. cinerea* spores. Expression levels were normalized to *Ubiquitin5* expression. The experiments were repeated three times with similar results. **B)** Representative pictures illustrating the morphology of vegetative rosettes of *SBT3.3* overexpressing plants and WT plants. **C)** The molar percentages of Fucose (Fuc), Rhamnose (Rha), Arabinose (Ara), Galactose (Gal), Glucose (Glu), Xylose (Xyl), Mannose (Man), Galacturonic Acid (Gal A) and Glucuronic Acid (Glc A) were quantified. The results represent the mean ± SD (n ≥ 3). Monosaccharide datasets are not significantly different according to analysis of variance (ANOVA) followed by Tukey's test ($P < 0.05$).

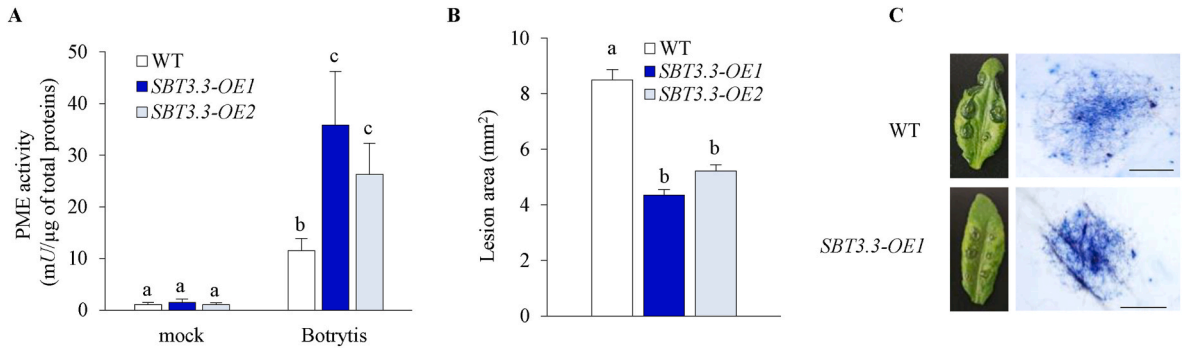

Fig. 5. Overexpression of *SBT3.3* in Arabidopsis overactivates PME activity restricting Botrytis infection. A) Leaves of WT and of *SBT3.3-OE* plants were inoculated with mock and Botrytis and PME activity was quantified at 24-h post inoculation. The results represent the mean ± SD (n = 6). **C)** Quantification of lesion areas produced by the spread of the fungus at 24 h post inoculation. Data represent mean ± SE (n = 36 lesions for each genotype). **D)** Photographs showing lesion areas produced by Botrytis on leaves of WT and *SBT3.3-OE1* plants (left) and photomicrographs showing Botrytis colonization revealed by trypan blue staining. Bars = 1 mm. The different letters in A, B and C indicate significantly different datasets according to ANOVA followed by Tukey's test ($P < 0.05$).

staining (Fig. 5C). All these results support a role for SBT3.3 as a trigger of PME activity in Arabidopsis immunity to Botrytis.

3.5. Modification of SBT3.3 expression in arabidopsis influences pectin methylester content and defense gene expression against Botrytis

Subsequently, we attempted to identify the molecular mechanism underlying the different susceptibility observed in *SBT3.3* expression-altered lines. To test whether the altered defense-related PME activity observed could lead to changes in CW methylesterification, the methylesters was quantified in leaves of *sbt3.3* mutants, *SBT3.3–OE* lines and WT plants at 24 h post *B. cinerea* inoculation. A significantly higher amount of methylester was detected in *sbt3.3* mutants than in WT plants while a significantly lower amount was revealed in *SBT3-3-OE* lines (Fig. 6). This result indicates that *SBT3.3* expression can influence CW methylesterification in plant defense. We next investigated the possibility that the improved resistance observed in *SBT3.3* over-expressing lines may also be related to a more robust immune response. The induction of a number of defense-related genes important for Arabidopsis immunity against Botrytis was compared between WT and *SBT3.3-OE1* plants inoculated with mock and Botrytis (Fig. 7). Interestingly, greater induction of *WRKY33*, *PAD3*, and *WAK2* was observed in *SBT3.3-OE1* plants compared to WT, when challenged with Botrytis (Fig. 7). *CYP81F2* showed similar expression levels in WT and *SBT3.3-OE1* plants. Instead, a lower induction of *pro-PME17* and *PMEI10* expressions was detected in *SBT3.3-OE1* line compared to WT. Considering the lower levels of *B. cinerea* β-tubulin and fungal symptoms observed in the transgenic plants (Figs. 7 and 5B and C), these results indicate that overexpression of *SBT3.3* can stimulate the expression of *WRKY33*, *PAD3, WAK2* and *CYP81F2* and not that of *pro-PME17* and *PMEI10*.

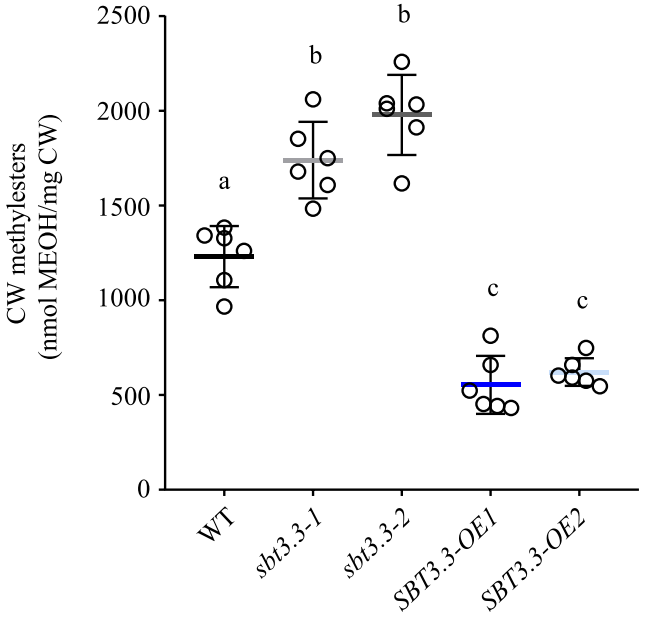

Fig. 6. The methyl ester content is altered in *sbt3.3* mutants and *SBT3.3–OE* lines. The amount of methyl esters in the cell wall was quantified 24 h after inoculation. Results represent mean ± SD (n = 6). The different letters on the bars indicate datasets significantly different according to ANOVA followed by Tukey's test ($P < 0.05$).

Leaves of WT, *sbt3.3–1*, *sbt3.5–1* and *SBT3.3-OE1* plant were inoculated with mock or *B. cinerea* and stained with 3,3′-diaminobenzidine (DAB) to reveal the accumulation of H_2O_2 in the tissue (Supplemental Fig. S4). No accumulation of H_2O_2 was observed in mock-inoculated leaves of all genotypes analyzed and a similar DAB staining was revealed in all leaves challenged with Botrytis.

3.6. SBT3.3 and pro-PME17 are secreted through distinct protein secretion pathways in the apoplast

With the aim of deepening our knowledge on the secretion patterns and on the final subcellular destination of SBT3.3 and its putative target pro-PME17, a fluorescent variant of the two proteins was constructed by fusing the respective encoding cDNA to *yfp* and *gfp,* under the control of *35S* promoter. The fluorescent tag was linked to the C-terminus of both proteins, since neither is predicted to have the ω site of the glycosylphosphatidylinositol (GPI) anchor addition (predGPI software; http://gpcr2.biocomp.unibo.it/predgpi/), as previously found for AtPMEI1 (De Caroli et al., 2011). The *SBT3.3-YFP* and *pro-PME17-GFP* constructs were transiently expressed in the epidermal cells of tobacco leaves and observed by laser scanning confocal microscopy (Fig. 8, Fig. 9 and Supplemental Fig. S5). Both proteins accumulated in the apoplast as confirmed by colocalization with the CW marker XTH11-RFP (De Caroli et al., 2021) (Fig. 8A–C and Fig. 9A–C) and plasmolysis of epidermal cells co-expressing both *pm-rk*, marker of plasma membrane and *SBT3.3-YFP* or *pro-PME17-GFP* (Figs. 8D and 9D). Nevertheless, the fluorescence signals related to SBT3.3-YFP and pro-PME17-GFP showed different secretion patterns. SBT3.3-YFP exhibited a typical cytosolic fluorescent pattern, labelling the nucleoplasm and appearing excluded by the ER and Golgi stacks, without any colocalization with the specific organelle markers, RFP-HDEL and ST52-mCherry, respectively (Nelson et al., 2007) (Fig. 8E–J). In addition to the nucleoplasm and CW, SBT3.3-YFP labelled small punctate cytosolic structures that

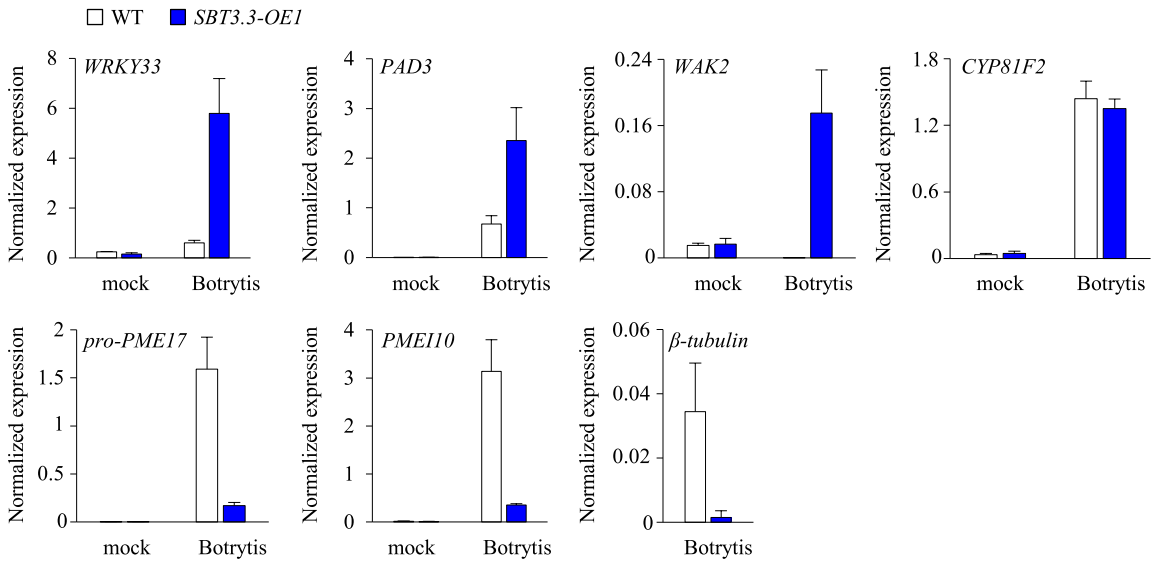

Fig. 7. *SBT3.3* overexpression enhances defense related gene expression in Arabidopsis during Botrytis infection. The induction of the expression of defense genes *WRKY33, PAD3, WAK2, CYP81F2, pro-PME17* and *PMEI10* were compared between *SBT3.3-OE1* line and WT plants challenged with Botrytis. The mRNA expression was analyzed at 24 hpi in *B. cinerea*- or mock-inoculated leaves by qPCR. Botrytis *β-tubulin* expression was also quantified. The expression levels were normalized to *Ubiquitin5* expression. The experiments were repeated three times with similar results.

significantly colocalized with the Exocyst Positive Organelles (EXPOs) marker Exo70E2-mCherry (Wang et al., 2010) indicating the possible involvement of EXPOs in an unconventional trafficking of the chimera toward the CW (Fig. 8K-M). Treatment with Brefeldin A (BFA), an inhibitor of ER-Golgi trafficking (Zhang et al., 2011) did not affect SBT3.3-YFP secretion pattern while it clearly perturbed the Golgi organization labelled by ST52-mCherry (Fig. 8N-P). A conventional secretion pathway is followed by pro-PME17-GFP that labelled the ER, continuous to the nuclear envelope, and small punctate structures that colocalize with the ER and the Golgi markers, respectively (Fig. 9E–J). Intriguingly, pro-PME17 reached the apoplast before the SBT3.3. At 48 h post transformation (hpt), the CW was intensely labelled by pro-PME17-GFP and, at approximately 60 hpt by SBT3.3-YFP protein fusion (Fig. 8A–C and Fig. 9A–C). These results indicate that both SBT3.3 and pro-PME17 are correctly secreted into the apoplast using different secretion pathways and in a temporally staggered manner. We further explored the timing of SBT3.3 and pro-PME17 colocalization into the CW using a *rfp*-tagged version of *pro-PME17,* under the control of *35S* promoter transiently co-expressed with *SBT3.3-YFP* in the epidermal cells of tobacco leaves. We confirmed that the pro-PME17 and SBT3.3 colocalize in CW, and this is favoured over time as revealed by colocalization parameters (Fig. 10).

4. Discussion

Plants exploit a great and local increase of PME activity in response to pathogens with different lifestyles (Lionetti, 2015; Lionetti et al., 2014). Here, intriguingly we note that all PME isoforms, induced in *A. thaliana* during *B. cinerea* infection, are organized as zymogens in which the catalytic region is preceded by an N-terminal pro region. The structural similarity revealed between the amino acid sequences of the pro regions of these PMEs and the immunity-related PMEIs (AtPMEI10 and AtPMEI11) support their possible role as intramolecular inhibitors in each specific pro-PME cluster (Del Corpo et al., 2020; Lionetti et al., 2017). We explored the possible role of SBTs as post-transcriptional regulators of PME activity in Arabidopsis immunity against the necrotrophic fungus *B. cinerea*. Exploiting publicly available microarray data, we selected two genes, *SBT3.3* and *SBT3.5* because they are induced in several Arabidopsis-pathogen interactions and in response to several elicitors of plant defense responses. Furthermore, they are co-expressed with the *pro-PME17* during Botrytis infection. We demonstrated that *SBT3.3* and *SBT3.5* are induced in Botrytis-challenged Arabidopsis leaves, with *SBT3.3* exhibiting greater fold-induction than *SBT3.5*. *SBT3.3* appeared to be particularly involved in plant defense because it is induced in leaves specifically during the infection process and participates in OG-induced signalling. Previous evidence indicates that *SBT3.3* expression responds very rapidly to H_2O_2 and it enhances the activation of mitogen-activated protein kinases (MAPKs) following microbial attack (Ramirez et al., 2013). All the evidence points to the involvement of SBT3.3 and SBT3.5 as important contributors in the activation of the earliest signalling events of PTI against Botrytis and several other pathogens.

The possible role of SBT3.3 and SBT3.5 as PME activators in Arabidopsis immunity against *B. cinerea* infection was explored. A significant lower induction of PME activity was observed in *B. cinerea*-infected *sbt3.3* and *sbt3.5* mutants compared to WT plants. The *sbt3.3–1*, *sbt3.3–2, sbt3.5–1*, *sbt3.5-2* mutants showed greater susceptibility to the fungus than WT. Our results indicate that the expression of *SBT3.3* and *SBT3.5* can influence the induction of defense-related PME activity and fungal invasion and suggest that SBT3.3 have a greater contribution on this induction. The two SBTs may directly contribute to the release of the pro region from pro-PMEs. The involvement of multiple SBT/pro-PME pairs is suggested by the variability in the processing motifs of the PME isoforms involved in Arabidopsis-Botrytis interaction. SBT3.5 can process pro-PME17 at the predictable RKLL motif (Senechal et al., 2014). The presence of this cleavage site in pro-PMEPCRA and pro-PME21 suggests these isoforms as further targets of SBT3.5. SBT3.3 could synergistically act with SBT3.5 to activate pro-PME17, perhaps by processing the additional cryptic processing site proposed in this isoform. More efforts are needed to understand the role of pro-PMEs processing motifs. The weaken resistance in *sbt* mutant lines might also be part of the pleiotropic effects related to the lack of *SBTs* expression rather than resulting directly from PME activity states. We revealed a significant higher induction of PME activity and higher Botrytis resistance in *SBT3.3-OE1* and *SBT3.3-OE2* infected leaves compared to untransformed plants. Overall, our evidence indicates that SBT3.3 and SBT3.5 can contribute to the activation of PME activity to counteract *B. cinerea* infection. The absence of growth abnormalities and of alterations in monosaccharide composition in *sbt* mutants and *SBT3.3-OE* lines indicates that, in leaves of adult plants, these SBTs are mainly

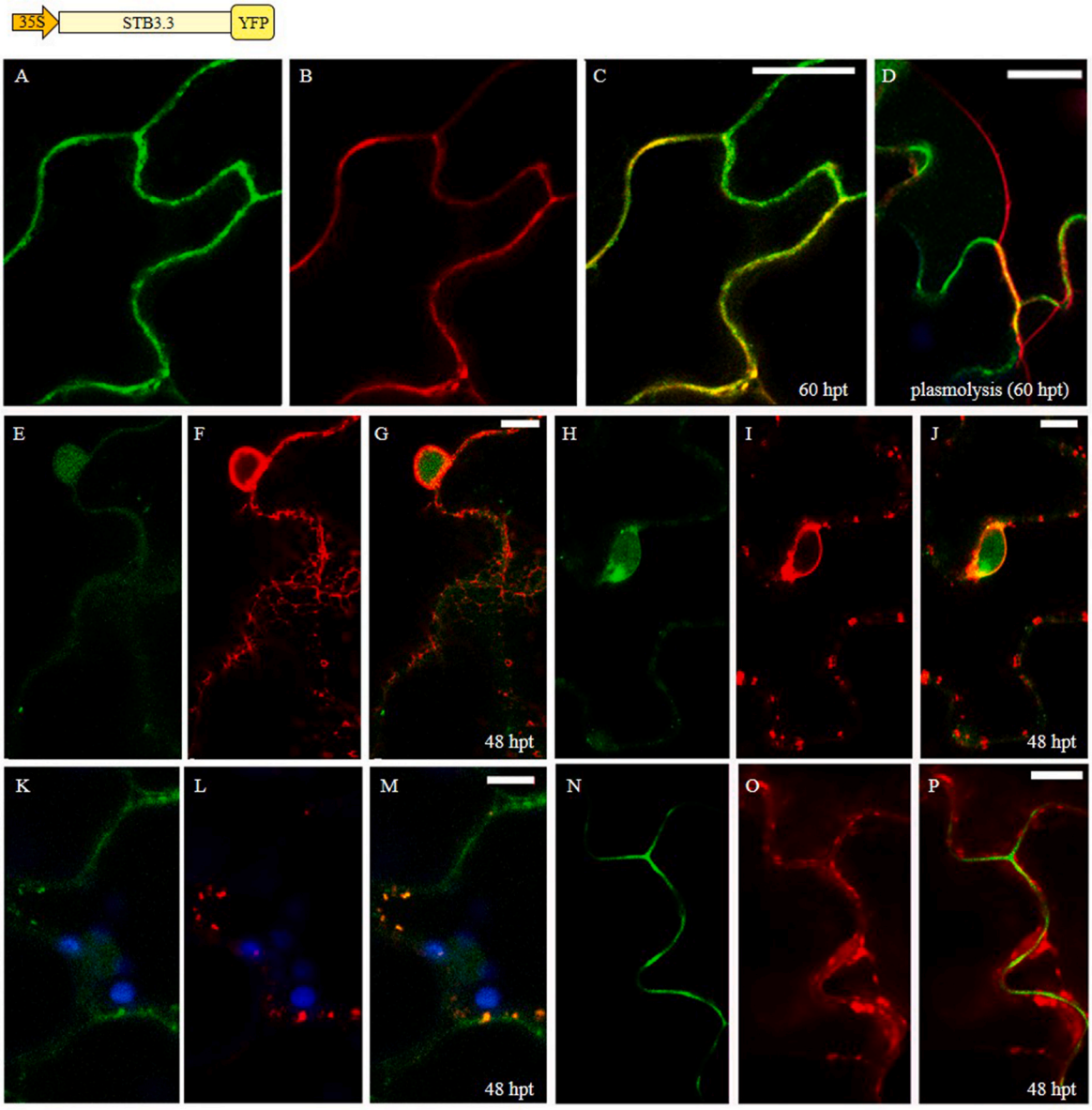

Fig. 8. SBT3.3 is delivered in the apoplast through an unconventional secretion pathway. Confocal microscopy images of epidermal cells of *Nicotiana tabacum* adult leaves showing the expression of (**A,E,H,K and N**) SBT3.3-YFP and its co-expression with different markers of subcellular compartments (**B–C:** XTH11-RFP, cell wall; **F-G:** RFP-HDEL, endoplasmic reticulum; **I-J:** ST52-mCherry, Golgi stacks; **K-M:** Exo70E2-mCherry, EXPOs) at the indicated hours post transformation (hpt). (**N–P**) After BFA treatment, SBT3.3-YFP fluorescent pattern does not change, while ST52-mCherry one appears perturbated. (**D**) Plasmolyzed cells (1 M NaCl) expressing SBT3.3-YFP and the plasma membrane marker pm-rk show the green fluorescent cell wall and the retracted red fluorescent plasma membrane. Chlorophyll autofluorescence within the chloroplasts is depicted in blue. Scale bars = 20 μm in A-C, 10 μm in E-P and 5 μm in D.

involved in immune processes.

The amount of CW methylesters negatively correlated with the level of *SBT3.3* expression and PME activity in the analyzed genotypes. SBTs, by promptly activating PMEs, could favour a pectin de-methylesterification, increasing the charged carboxyl groups that may form Ca^{2+}-mediated pectin crosslinks to strengthen the CW structure and resistance to the microbe. In addition to a structural contribution, our data indicate that SBT3.3 contributes to an immune gene activation against Botrytis. The overactivation of *WRKY33*, *PAD3*, *CYP81F2* and *WAK2* genes in *SBT3.3-OE1* unveils a more robust immune response to Botrytis, including the production of antimicrobial compounds such as camalexin, indole glucosinolates (Birkenbihl et al., 2012) and enhanced CW integrity surveillance. *WAK2* is a wall-associated kinase that requires PME activity to activate OGs-dependent stress responses (Kohorn et al., 2014). It can be assumed that SBT3.3 could promote WAK2-pectin binding and WAK2-OG-mediated stress signalling. Our evidence together with previous results indicate that OGs induce the expression of *SBT3.3, WRKY33, PAD3* and *CYP81F2* and that SBT3.3 can self-activate (Denoux et al., 2008; Ramirez et al., 2013). A positive feedback loop based on PME activity and production of active OGs, could be mounted to strengthen the activation of OGs-mediated defense responses. Moreover, an appropriate degree of methylesterification seems critical for the OGs release and/or for the elicitation of an OG-mediated defense response (Lionetti et al., 2012). Partially de-methylesterified OGs is required to elicit defense responses in *Fragaria vesca* fruits (Osorio et al., 2008). OGs with different methylesterification status were detected in Arabidopsis–Botrytis interaction (Voxeur et al., 2019). The possibility that SBTs, pro-PMEs and PMEIs can serve to finely tune the release, the activity, and the perception of OGs for an efficient signalling activation in priming is an interesting hypothesis to be investigated.

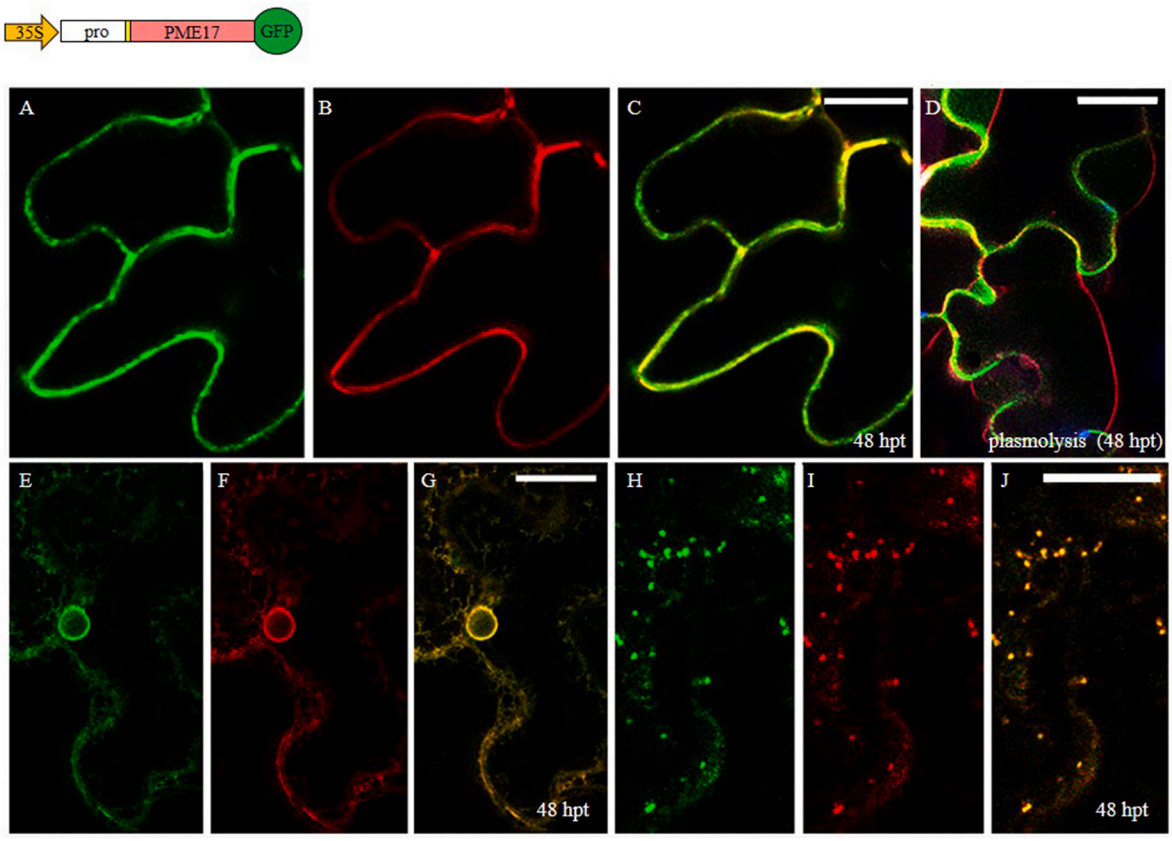

Fig. 9. Pro-PME17 is delivered in the apoplast through a conventional secretion pathway. Confocal microscopy images of epidermal cells of *Nicotiana tabacum* adult leaves showing the expression of (**A, E and H**) pro-PME17-GFP and its co-expression with different markers of subcellular compartments (**B–C:** XTH11-RFP, cell wall; **F-G:** RFP-HDEL, endoplasmic reticulum; **I-J:** ST52-mCherry, Golgi stacks) at the indicated hours post transformation (hpt). (**D**) Plasmolyzed cells (1 M NaCl) expressing pro-PME17-GFP and the plasma membrane marker pm-rk show the green fluorescent cell wall and the retracted red fluorescent plasma membrane. Chlorophyll autofluorescence within the chloroplasts is depicted in blue. Scale bars = 20 μm in A-C, 10 μm in E-J, and 5 μm in D.

SBTs-dependent PME activity could also favour the binding and the functions of other PRR, like WAK1 and FERONIA, known to preferentially bind de-methylesterified crosslinked pectins. All these observations could imply that SBTs and PME activities exploit a cooperation between CW integrity maintenance and PTI signalling to regulate defense responses after a CW damage (Swaminathan et al., 2022). Proteases could target multiple substrates and the possibility that the resistance phenotypes observed in the *SBT3.3-OE* lines could be the result of synergy between activation of pro-PMEs and other precursors should also be considered. Our results indicate also that SBTs expression does not alter H_2O_2 accumulation, an important defense response to Botrytis infestation (Pogorelko et al., 2013; Reem et al., 2016).

SBT3.3 was previously found in the extracellular compartment, but its secretion pathway was never explored (Ramirez et al., 2013). Pro-PME17 was predicted as apoplastic protein, but its localization was never demonstrated. In this study, we also provide insights into SBT3.3 and pro-PME17 targeting and subcellular localization. While pro-PME17 follows a conventional secretion pathway, SBT3.3 undergoes an Unconventional Protein Secretion (UPS) as it bypasses the Golgi, is insensitive to BFA, and colocalizes with Exo70E2, a subunit of the exocyst complex specifically identified in EXPOs involved in unconventional exocytosis. To date, SAMS2, involved in lignin methylation and XTH29, an endotransglucosylase/hydrolases, are the two CW proteins reported to be secreted as EXPO cargo (De Caroli et al., 2021; Wang et al., 2010). EXPO-mediate secretion emerges as a toolkit exploited by plants to ensure a dynamic remodelling of the CW structure capable of adapting to environmental changes and growing conditions. Furthermore, pro-PME17 reaches the CW earlier than SBT3.3 and their colocalization in the apoplast increases over time. Assuming an interaction between the two proteins, the spatio-temporal separations could avoid a premature PME activation and pectin de-methylesterification during the secretion into the CW. Plants could accumulate inactive pro-PMEs clusters on the cell surface to be rapidly activated by SBTs at the right time to amplify CW integrity signalling to promptly counteract pathogens. This proposed SBTs function would also be in line with de-repression accelerating the responsiveness of hormonal transcription networks in plants (Rosenfeld et al., 2002). The speed of a biotic stress defense response can be crucial for the survival of the sessile plant. In a similar mechanism, known as ectodomain shedding, proteolytic cleavage of extracellular domains of cell surface proteins results in the activation of a variety of normal and pathological signalling processes in animals (Paulus and Van der Hoorn, 2019). It is important to mention that SBTs are also pro-enzymes. Much effort is still needed to demonstrate these proposed mechanisms and to unravel the underlying regulators. Interestingly, SBT3.3 was involved in "priming", a sensory state able to induce a resistance faster and stronger respect to the same stimulus received before (Ramirez et al., 2013). *SBT3.3* expression mediates the activation of chromatin remodelling of defense genes including a self-activation, suggesting a positive feedback loop to potentiate the defense response and keep cells in a sustained sensitised mode. Our observation on the localization of SBT3.3-YFP in the nucleus can be consistent with this proposed role for SBT3.3. Moreover, it was previously hypothesized that "priming" could involve the accumulation of inactive proteins that becomes operative to initiate a signal amplification leading to a faster and stronger activation of defense responses. SBTs-mediated activation of pro-PMEs could be part of immune priming processes.

In conclusion, this study brings new insights into the molecular

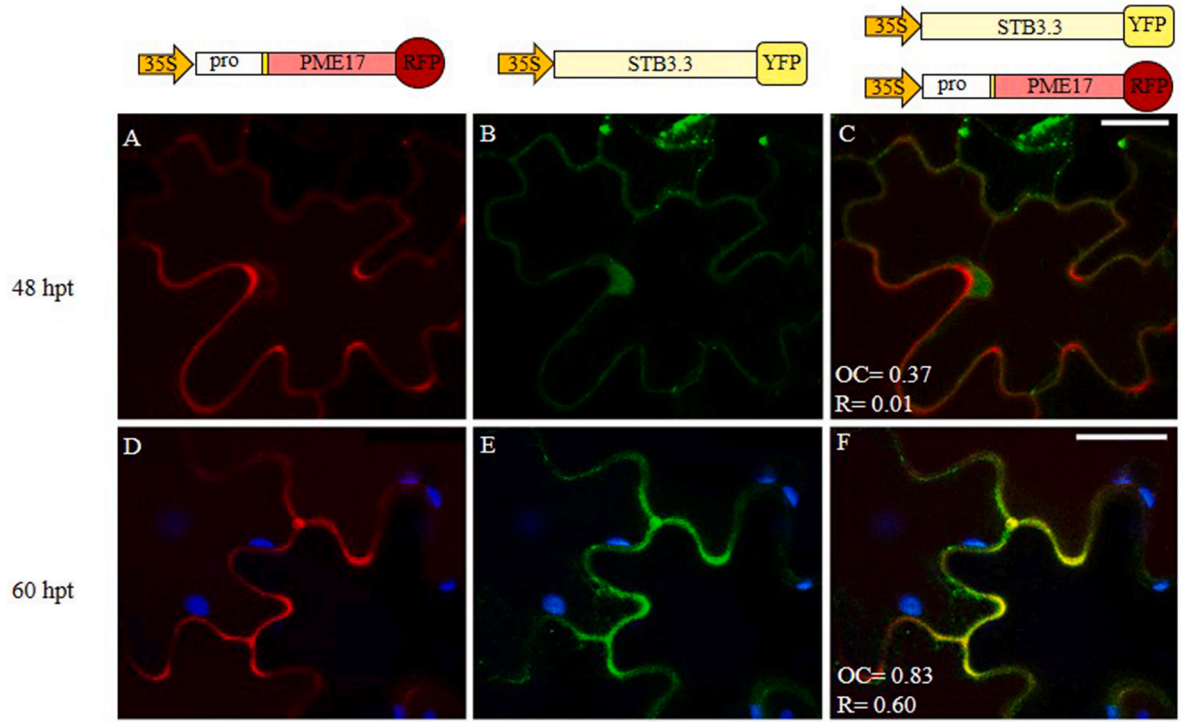

Fig. 10. Pro-PME17 and SBT3.3 colocalize in the cell wall and their colocalization is favoured over time. Confocal microscopy images of epidermal cells of tobacco adult leaves co-expressing pro-PME17-RFP (**A** and **D**) and SBT3.3-YFP (**B** and **E**) at the indicated hours post transformation (hpt). Merged images showing the co-localization of SBT3.3-YFP and pro-PME17-RFP in the cell wall (**C** and **F**). Overlap coefficient (OC, after Manders) and R (Pearson's correlation coefficient) values are reported in each merged image. Chlorophyll autofluorescence within the chloroplasts is depicted in blue. Scale bars = 20 μm.

mechanisms underlying the PME activation against necrotrophs. We propose SBT3.3 and SBT3.5 as factors modulating defense related PME activity and immune responses in Arabidopsis against pathogens. Biochemical evidence of pro-PME processing by SBTs and studies aimed at identifying SBT/pro-PME interactions will be needed to confirm a direct enzymatic proteolytic effect and identify SBT3.3/pro-PMEs pairs involved in plant immunity. SBT-mediated activation of PMEs can be exploited as an effective genomic tool to engineer long-lasting, broad-spectrum plant disease resistance and to avoid trade-offs between growth and defense.

Funding

The work was supported by Sapienza University of Rome, Grants RM120172B78CFDF2, RM11916B7A142CF1, RM122181424F1F42, RG12117A898EABE0 and to VL and AR12117A8A4A1ADC to DC.

Declaration of competing interest

The authors declare that they have no known competing financial interests or personal relationships that could have appeared to influence the work reported in this paper.

Data availability

Data will be made available on request.

Acknowledgments

We thank Marco Greco, Giamarco Tomassetti and Gabriele Pecatelli for technical assistance.

Appendix A. Supplementary data

Supplementary data to this article can be found online at https://doi.org/10.1016/j.plaphy.2023.107865.

References

Birkenbihl, R.P., Diezel, C., Somssich, I.E., 2012. Arabidopsis WRKY33 is a key transcriptional regulator of hormonal and metabolic responses toward Botrytis cinerea infection. Plant Physiol. 159, 266–285. https://doi.org/10.1104/pp.111.192641.

Brutus, A., Sicilia, F., Macone, A., Cervone, F., De Lorenzo, G., 2010. A domain swap approach reveals a role of the plant wall-associated kinase 1 (WAK1) as a receptor of oligogalacturonides. Proc. Natl. Acad. Sci. U.S.A. 107, 9452–9457. https://doi.org/10.1073/pnas.1000675107.

Coculo, D., Lionetti, V., 2022. The plant invertase/pectin methylesterase inhibitor superfamily. Front. Plant Sci. 13, 863892 https://doi.org/10.3389/fpls.2022.863892.

De Caroli, M., Lenucci, M.S., Di Sansebastiano, G.P., Dalessandro, G., De Lorenzo, G., Piro, G., 2011. Protein trafficking to the cell wall occurs through mechanisms distinguishable from default sorting in tobacco. Plant J. 65, 295–308.

De Caroli, M., Manno, E., Piro, G., Lenucci, M.S., 2021. Ride to cell wall: Arabidopsis XTH11, XTH29 and XTH33 exhibit different secretion pathways and responses to heat and drought stress. Plant J. 107, 448–466. https://doi.org/10.1111/tpj.15301.

Del Corpo, D., Fullone, M.R., Miele, R., Lafond, M., Pontiggia, D., Grisel, S., Kieffer-Jaquinod, S., Giardina, T., Bellincampi, D., Lionetti, V., 2020. AtPME17 is a functional Arabidopsis thaliana pectin methylesterase regulated by its PRO region that triggers PME activity in the resistance to Botrytis cinerea. Mol. Plant Pathol. 21, 1620–1633. https://doi.org/10.1111/mpp.13002.

Denoux, C., Galletti, R., Mammarella, N., Gopalan, S., Werck, D., De Lorenzo, G., Ferrari, S., Ausubel, F.M., Dewdney, J., 2008. Activation of defense response pathways by OGs and Flg22 elicitors in Arabidopsis seedlings. Mol. Plant 1, 423–445. https://doi.org/10.1093/mp/ssn019.

Dorokhov, Y.L., Komarova, T.V., Petrunia, I.V., Frolova, O.Y., Pozdyshev, D.V., Gleba, Y. Y., 2012. Airborne signals from a wounded leaf facilitate viral spreading and induce antibacterial resistance in neighboring plants. PLoS Pathog. 8.

Giovannoni, M., Lironi, D., Marti, L., Paparella, C., Vecchi, V., Gust, A.A., De Lorenzo, G., Nürnberger, T., Ferrari, S., 2021. The Arabidopsis thaliana LysM-containing Receptor-Like Kinase 2 is required for elicitor-induced resistance to pathogens. Plant Cell Environ. 44, 3775–3792. https://doi.org/10.1111/pce.14192.

He, Z., Webster, S., He, S.Y., 2022. Growth-defense trade-offs in plants. Curr. Biol. 32, R634–R639. https://doi.org/10.1016/j.cub.2022.04.070.

Hou, S., Jamieson, P., He, P., 2018. The cloak, dagger, and shield: proteases in plant–pathogen interactions. Biochem. J. 475, 2491–2509. https://doi.org/10.1042/BCJ20170781.

Hou, S., Liu, D., He, P., 2021. Phytocytokines function as immunological modulators of plant immunity. Stress Biology 1, 8. https://doi.org/10.1007/s44154-021-00009-y.

Kohorn, B.D., Kohorn, S.L., Saba, N.J., Martinez, V.M., 2014. Requirement for pectin methyl esterase and preference for fragmented over native pectins for wall-associated kinase-activated, EDS1/PAD4-dependent stress response in Arabidopsis. J. Biol. Chem. 289, 18978–18986.

Lin, W., Tang, W., Pan, X., Huang, A., Gao, X., Anderson, C.T., Yang, Z., 2021. Arabidopsis pavement cell morphogenesis requires FERONIA binding to pectin for activation of ROP GTPase signaling. Current Biology S096098222101589X. https://doi.org/10.1016/j.cub.2021.11.030.

Lionetti, V., 2015. PECTOPLATE: the simultaneous phenotyping of pectin methylesterases, pectinases, and oligogalacturonides in plants during biotic stresses. Front. Plant Sci. 6, 1–8.

Lionetti, V., Cervone, F., Bellincampi, D., 2012. Methyl esterification of pectin plays a role during plant-pathogen interactions and affects plant resistance to diseases. J. Plant Physiol. 169, 1623–1630.

Lionetti, V., Fabri, E., De Caroli, M., Hansen, A.R., Willats, W.G., Piro, G., Bellincampi, D., 2017. Three pectin methyl esterase inhibitors protect cell wall integrity for immunity to Botrytis. Plant Physiol. 173, 1844–1863. https://doi.org/10.1104/pp.16.01185.

Lionetti, V., Francocci, F., Ferrari, S., Volpi, C., Bellincampi, D., Galletti, R., D'Ovidio, R., De Lorenzo, G., Cervone, F., 2010. Engineering the cell wall by reducing de-methyl-esterified homogalacturonan improves saccharification of plant tissues for bioconversion. Proc. Natl. Acad. Sci. U.S.A. 107, 616–621. https://doi.org/10.1073/pnas.0907549107.

Lionetti, V., Raiola, A., Camardella, L., Giovane, A., Obel, N., Pauly, M., Favaron, F., Cervone, F., Bellincampi, D., 2007. Overexpression of pectin methylesterase inhibitors in Arabidopsis restricts fungal infection by Botrytis cinerea. Plant Physiol. 143, 1871–1880. https://doi.org/10.1104/pp.106.090803.

Lionetti, V., Raiola, A., Cervone, F., Bellincampi, D., 2014. Transgenic expression of pectin methylesterase inhibitors limits tobamovirus spread in tobacco and Arabidopsis. Mol. Plant Pathol. 15, 265–274.

Meyer, M., Huttenlocher, F., Cedzich, A., Procopio, S., Stroeder, J., Pau-Roblot, C., Lequart-Pillon, M., Pelloux, J., Stintzi, A., Schaller, A., 2016. The subtilisin-like protease SBT3 contributes to insect resistance in tomato. EXBOTJ 67, 4325–4338. https://doi.org/10.1093/jxb/erw220.

Nelson, B.K., Cai, X., Nebenfuhr, A., 2007. A multicolored set of in vivo organelle markers for co-localization studies in Arabidopsis and other plants. Plant J. 51, 1126–1136.

Osorio, S., Castillejo, C., Quesada, M.A., Medina-Escobar, N., Brownsey, G.J., Suau, R., Heredia, A., Botella, M.A., Valpuesta, V., 2008. Partial demethylation of oligogalacturonides by pectin methyl esterase 1 is required for eliciting defence responses in wild strawberry (Fragaria vesca). Plant J. 54, 43–55. https://doi.org/10.1111/j.1365-313X.2007.03398.x.

Paulus, J.K., Van der Hoorn, R.A.L., 2019. Do proteolytic cascades exist in plants? J. Exp. Bot. 70, 1997–2002. https://doi.org/10.1093/jxb/erz016.

Pelloux, J., Rustérucci, C., Mellerowicz, E.J., 2007. New insights into pectin methylesterase structure and function. Trends Plant Sci. 12, 267–277. https://doi.org/10.1016/j.tplants.2007.04.001.

Pogorelko, G., Lionetti, V., Fursova, O., Sundaram, R.M., Qi, M.S., Whitham, S.A., Bogdanove, A.J., Bellincampi, D., Zabotina, O.A., 2013. Arabidopsis and brachypodium distachyon transgenic plants expressing Aspergillus nidulans acetylesterases have decreased degree of polysaccharide acetylation and increased resistance to pathogens. Plant Physiol. 162, 9–23.

Pontiggia, D., Ciarcianelli, J., Salvi, G., Cervone, F., De Lorenzo, G., Mattei, B., 2015. Sensitive detection and measurement of oligogalacturonides in Arabidopsis. Front. Plant Sci. 6 https://doi.org/10.3389/fpls.2015.00258.

Ramirez, V., Lopez, A., Mauch-Mani, B., Gil, M.J., Vera, P., 2013. An extracellular subtilase switch for immune priming in Arabidopsis. PLoS Pathog. 12, e1006003 https://doi.org/10.1371/journal.ppat.1006003.

Rautengarten, C., Usadel, B., Neumetzler, L., Hartmann, J., Büssis, D., Altmann, T., 2008. A subtilisin-like serine protease essential for mucilage release from Arabidopsis seed coats. Plant J. 54, 466–480. https://doi.org/10.1111/j.1365-313X.2008.03437.x.

Reem, N., Pogorelko, G., Lionetti, V., Chambers, L., Held, M.A., Bellincampi, D., Zabotina, O.A., 2016. Decreased polysaccharide feruloylation compromises plant cell wall integrity and increases susceptibility to necrotrophic fungal pathogens. Front. Plant Sci. 7, 630. https://doi.org/10.3389/fpls.2016.00630.

Rosenfeld, N., Elowitz, M.B., Alon, U., 2002. Negative autoregulation speeds the response times of transcription networks. J. Mol. Biol. 323, 785–793. https://doi.org/10.1016/s0022-2836(02)00994-4.

Schaller, A., Stintzi, A., Rivas, S., Serrano, I., Chichkova, N.V., Vartapetian, A.B., Martínez, D., Guiamét, J.J., Sueldo, D.J., van der Hoorn, R.A.L., Ramírez, V., Vera, P., 2018. From structure to function - a family portrait of plant subtilases. New Phytol. 218, 901–915. https://doi.org/10.1111/nph.14582.

Senechal, F., Graff, L., Surcouf, O., Marcelo, P., Rayon, C., Bouton, S., Mareck, A., Mouille, G., Stintzi, A., Hofte, H., Lerouge, P., Schaller, A., Pelloux, J., 2014. Arabidopsis PECTIN METHYLESTERASE17 is co-expressed with and processed by SBT3.5, a subtilisin-like serine protease. Ann. Bot. 114, 1161–1175.

Swaminathan, S., Lionetti, V., Zabotina, O.A., 2022. Plant cell wall integrity perturbations and priming for defense. Plants 11, 3539. https://doi.org/10.3390/plants11243539.

Tornero, P., Conejero, V., Vera, P., 1996. Primary structure and expression of a pathogen-induced protease (PR-P69) in tomato plants: similarity of functional domains to subtilisin-like endoproteases. Proc. Natl. Acad. Sci. USA 93, 6332–6337. https://doi.org/10.1073/pnas.93.13.6332.

Voxeur, A., Habrylo, O., Guénin, S., Miart, F., Soulié, M.-C., Rihouey, C., Pau-Roblot, C., Domon, J.-M., Gutierrez, L., Pelloux, J., Mouille, G., Fagard, M., Höfte, H., Vernhettes, S., 2019. Oligogalacturonide production upon Arabidopsis thaliana–Botrytis cinerea interaction. Proc. Natl. Acad. Sci. USA 116, 19743–19752. https://doi.org/10.1073/pnas.1900317116.

Wang, Juan, Ding, Y., Wang, Junqi, Hillmer, S., Miao, Y., Lo, S.W., Wang, X., Robinson, D.G., Jiang, L., 2010. EXPO, an exocyst-positive organelle distinct from multivesicular endosomes and autophagosomes, mediates cytosol to cell wall exocytosis in Arabidopsis and tobacco cells[C][W]. Plant Cell 22, 4009–4030. https://doi.org/10.1105/tpc.110.080697.

Wolf, S., Rausch, T., Greiner, S., 2009. The N-terminal pro region mediates retention of unprocessed type-I PME in the Golgi apparatus. Plant J. 58, 361–375. https://doi.org/10.1111/j.1365-313X.2009.03784.x.

Zhang, H., Zhang, L., Gao, B., Fan, H., Jin, J., Botella, M.A., Jiang, L., Lin, J., 2011. Golgi apparatus-localized synaptotagmin 2 is required for unconventional secretion in Arabidopsis. PLoS One 6, e26477. https://doi.org/10.1371/journal.pone.0026477.

Zhou, J.-M., Zhang, Y., 2020. Plant immunity: danger perception and signaling. Cell 181, 978–989. https://doi.org/10.1016/j.cell.2020.04.028.